Journal Title
XX(X):1–8

DOI: 10.1177/ToBeAssigned
www.sagepub.com/
SAGE

Modelling Weather Dependence in Online Reliability Assessment of Power Systems

**Samuel Perkin[1,2], Arne Brufladt Svendsen[3], Trond Tollefsen[3], Ingrid Honve[4]
Iris Baldursdottir[2], Hlynur Stefansson[1], Ragnar Kristjansson[1] and Pall Jensson[1]**

Abstract

Probabilistic reliability assessment of power systems is an ongoing field of research, particularly in the development of tools to model the probability of exogenous threats, and their potential consequences. This paper applies a weather-dependent failure rate model to a region of the Icelandic transmission system, using 10 years of weather data and overhead line fault records. The studied failure rate model is compared with a constant failure rate model, in terms of variability and how well the models perform in a blind test over a 2 year period in reflecting the occurrence of outages. The weather-dependent and constant failure rate models are then used as input to a state-of-the-art risk assessment tool to determine the sensitivity of such software to weather-dependent threats. The results show the importance of weather-dependent contingency probabilities in risk estimation, and in quantitative assessment of maintenance activities. The results also show that inclusion of weather-dependence in power system reliability assessments affects the overall distribution of risk, as a positively-skewed distribution with high risk periods occurring at low frequency.

Keywords

Environmental risk, failure data analysis, network reliability, probabilistic methods, system simulation

Introduction

The study of power system reliability is based on the fundamental works of Endrenyi (1978) and Billinton and Allan (1996), although probabilistic methods have been actively studied since 1947 as shown by Billinton (1972). Traditionally, Transmission System Operators (TSOs) have managed the reliability of their power system by applying an interpretation of the N-1 criterion, as discussed in GARPUR consortium (2014*b*), based on ENTSO-E (2009). In general, the N-1 criterion requires that the power system remains in an secure state following the failure or outage of any single major component (overhead lines, cables, transformers, generators), and that they have no impact outside the TSO's responsible area. As such, TSOs managed reliability by building redundancy into their system to manage discrete outages. Historically, large-scale blackouts have occurred due to multiple component outages occurring at the same time (e.g. due to severe weather), or line overloads and voltage collapses following an initial fault Pourbeik et al. (2006). Modern power systems are now facing greater uncertainty in operation, with the increased liberalization of markets and increased penetration of intermittent power sources, such as wind and solar. The risks associated with this uncertainty, as well as the bunching of faults due to weather, cannot be effectively managed by the N-1 criterion.

The dominant method for determining the probability of contingencies (sudden component outages) is through the use of failure rate models Billinton and Allan (1996). Failure rates are either calculated for individual, or groups of similar, components and have been historically reported in grid studies as constant values Bollen (1993). In the last couple of decades a large number of papers have developed variable failure rates to model the influence of weather, maintenance, sustained stress, and other external threats to the system. The effect of weather on the probability of outages is especially emphasised Kirschen and Jayaweera (2007), Alvehag and Soder (2011) and Billinton and Acharya (2006). Although a number of failure rate models exist, they are not yet commonly used by TSOs GARPUR consortium (2014*b*).

Present day research has not yet extensively studied the sensitivity of failure rate models and reliability assessment tools when applied to real-world power systems, under realistic data availability limitations. The cost of high-resolution spatio-temporal data required to perform probabilistic reliability assessments is a barrier to their implementation, and therefore studies like the one performed in this paper are required in order to eventually estimate the value of investing in such data.

The next section, backround, discusses relevant papers related to failure rate models and reliability assessment, and TSO experiences with software related to probabilistic reliability assessment. The failure rate modelling section describes an extension of the model described in Tollefsen et al. (2015). The failure rate model is extended to include

[1] Reykjavik University, Reykjavik, Iceland
[2] Landsnet, Reykjavik, Iceland
[3] Goodtech Power, Bergen, Norway
[4] Webstep, Bergen, Norway

Corresponding author:
Samuel Perkin, Landsnet, Gylfaflot 9, 112 Reykjavik, Iceland
Email: samuelp@landsnet.is

the threat of icing, to validate and extend a prior case-study of Perkin et al. (2016). The failure rate comparison section applies the extended model to a region of the Icelandic transmission system, comparing it with a constant failure rate model. This is followed by a section on how the use of variable failure rate models affects system risk assessments, compared to constant failure rate models, to highlight the importance of capturing weather-dependence in reliability assessments.

Background

Failure rate models can be broadly classified into state-based Billinton and Wenyuan (1991) and threat-based Vefsnmo et al. (2015) models, as discussed in previous work Perkin et al. (2016). A further level of classification can be made between models that are based on individual components or sub-components (e.g. single spans of overhead lines) and models that aggregate fault statistics for a given type of component as in Bollen (1993). The latter type of model is applicable to transmission systems that have a large number of similar components that experience similar environmental threats, whilst the former is applicable to systems in which threats, and their likelihood, vary greatly from line to line.

A large body of research on online reliability assessment has previously identified the need to move towards probabilistic methods due to the threats caused by the exogenous environment GARPUR consortium (2014*a*). Some recent contributions to the field of probabilistic reliability assessment include Henneaux and Kirschen (2016), Karangelos and Wehenkel (2016) and Zhang et al. (2015). A review of both academic and commercial tools can be found in GARPUR consortium (2014*b*). The recently finished iTesla project aimed at short-term operation with a new security assessment tool able to cope with increasing uncertainty and takes advantage of new grid technologies and flexible operating procedures Lemaitre and Panciatici (2014). In UMBRELLA consortium (2016), the UMBRELLA project makes a number of recommendations, including the need for risk-based criteria and tools to be developed at European TSOs. Beyond the problem of reliability assessment, there is an additional body of research on optimising the reliability of the power system through control, covered by the literature review of Capitanescu (2016). An example of a TSO application of security-constrained optimal power flow (SCOPF) models is provided in López et al. (2015). Such SCOPF models may be eventually modified to replace the determinstic N-1 set of contingencies with a dynamic probabilistic set of contingencies.

One of the few commercially available tools for online probabilistic reliability assessment is Promaps (PRObability Method Applied to Power System). This online tool calculates the power system's reliability as a function of power demand and system topology, for use in real-time operation Digernes et al. (2007). The simulation also takes into account the probability of failure of all N-1 faults and most N-2 faults. Input to the software is a live export of the system state from the TSO's SCADA system every 5-10 minutes. The reliability technique in Promaps is based on Markov unit models that represent each component. The tool uses Kronecker products to aggregate components to reduce the size of each subsystem and the total system state space, without reducing the information. This is combined with a load flow model that minimizes a cost function representing the system's impedance. The simulation tool has been developed through a 5 year R&D project financed by Statnett in Norway. The simulation tool is currently in operation for the Norwegian TSO Statnett, the Icelandic TSO Landsnet and the Norwegian DSO Hafslund. Later in this paper, the sensitivity of the Promaps online tool to weather-dependent failure rate models is investigated.

TSO feedback from Landsnet and Statnett on the Promaps online software strongly suggests the need for weather-dependent failure rates. By only using constant failure rates, probabilistic reliability assessments fail to model exogenous threats to the system, such as icing, wind, lightning, snow, and sabotage. As such the reliability will be over-estimated in bad weather, and under-estimated in good weather. This is corrected by modelling variable failure rates that are fitted to historical weather data, and can then estimate outage probabilities given some weather observation. Both Statnett and Landsnet independently concluded that linking weather to reliability via failure rates would be a significant improvement to Promaps. Hence, the motivation for this paper is to achieve this enhanced model, and to provide a preliminary assessment of its impact on reliability indices.

The experience of the Portuguese TSO with applying threat-based failure rate models to their system is outlined and discussed in Azevedo et al. (2015) and Machado et al. (2014). Notably the set of threats considered on the Portuguese system is quite different to those experienced in Iceland as outlined by Eliasson (2005). A theoretical study on outages caused by icing on the Icelandic system is made in Perkin et al. (2016), which is extended on in this paper, as well as a study on the influence of wind on the Norwegian system in Tollefsen et al. (2015). There are few published studies on threat probabilities to real-world power systems, due to both security concerns as well as there being no historical need for probabilistic models due to the deterministic N-1 criterion being sufficient for power system reliability. As discussed in Panciatici et al. (2012), there is a growing perception that the N-1 criterion is no longer sufficient for ensuring the reliability of modern power systems, and hence there is now a need to develop and implement probabilistic reliability methods.

Failure rate modelling

This paper applies an extension of the weather-dependent failure rate model in Tollefsen et al. (2015) to the Icelandic power system. This model is compared with constant failure rate models, which are presently calculated as a metric of long-term component reliability. This section outlines the data used and the modelling methods that were applied, and then makes a direct comparison between the two models.

Data

At minimum, the calculation of failure rates requires a time-series of outages, for each component. For ease of notation, the following equations refer to only a single component. In order to use threat-based failure rate models, each outage must be accompanied by an indication of the threat that induced the outage. We define the outage data, F, of N outages for a single component as

$$F = \{(t_1, \psi_1, r_1), ..., (t_N, \psi_N, r_1)\} \quad (1)$$

Where t_j, ψ_j and r_j define the j^{th} time of occurrence, the underlying threat and the duration of the outage, respectively.

This study considers the reliability of seven overhead transmission lines in a region of the Icelandic power system, for which there exists outage statistics over the past 26 year period. As noted in Eliasson (2005), wind and ice loading are two main threats to the overhead transmission lines in Iceland. The credible threats, k, considered in this study are:

(a $k = 0$: Other;

(b $k = 1$: Wind with no ice load;

(c $k = 2$: Wind with ice load.

The 'other' category contains threats that weren't identified to be influenced by wind or ice loading, or were of unknown cause. Note that the three threats are defined such that they are mutually exclusive.

Given F and the definition of threats, we can define a time-series, $x_{k,t}$, which is equal to 1 when $t = t_j$ and $\psi_j = k$ for some outage j, and equal to 0 otherwise. This time series therefore denotes an indicator of the time periods t in which the component has experienced an outage due to threat k.

The weather data used for this study consists of a time-series of wind and ice loading at two locations in the studied region. General weather data was generated using historical observational data and the Weather Research and Forecasting (WRF) model. The ice load time-series was produced by a model based upon Makkonen (2000). The weather data set, W, is defined as

$$W = \{(w_1, i_1), ..., (w_T, i_T)\} \quad (2)$$

Where w_j and i_j represent the j^{th} average hourly wind speed in metres per second, and estimated hourly ice growth in kilograms per metre of overhead line, respectively.

Models

This paper compares two failure rate models, a constant failure rate model and an extension of the model presented in Tollefsen et al. (2015). The constant failure rate model is calculated using the method described in Billinton and Allan (1992). Given the description of fault statistics above, the constant failure rate can be estimated as

$$\bar{\lambda} = \frac{\sum_k \sum_t x_{k,t}}{(T - \sum_j r_j)} \quad (3)$$

Which is the sum of all outages due to all faults, divided by the uptime of the component. The term in the denominator, $\sum_j r_j$, subtracts the total downtime of the component from its lifetime. The downtime must be subtracted given that a component can't fail in hours that it is not already operational.

The weather-dependent model in Tollefsen et al. (2015) correlated faults to wind speed. The extension of this model includes the influence of icing on overhead line failures, given that icing constitutes a significant threat to the Icelandic transmission system. The basic structure of the model is

$$\lambda_t = \lambda_0 + (1 - \beta_t)c_{1,s}\lambda_1 + \beta_t c_{2,s}\lambda_2 \quad (4)$$

Where λ_0, λ_1, and λ_2 are the failure rates for 'other', 'wind with no ice load', and 'wind with ice load' faults, respectively. The term β_t is a binary indicator variable that defines whether icing is credible in a given hour. This is calculated using the ice load data as

$$\beta_t = \begin{cases} 1, & \text{for } i_t \geq 0 \quad (5) \\ 0, & \text{otherwise} \quad (6) \end{cases}$$

The remaining two multipliers, $c_{1,s}$ and $c_{2,s}$ are the wind correction factors, which are a function of the wind speed experienced by the component at time t. There are two correction factors to separate the case of a line without ice load from the case where a line may be experiencing icing.

These correction factors first require the normalization of all wind speeds with the 99$^{\text{th}}$ percentile wind speed (from now w_{99} as short). The wind speeds are then separated into eight discrete categories defined in Table 1. Therefore, at some point in time t the wind speed can be mapped to a wind category, $w_t \mapsto s$ which then identifies the relevant correction factor $c_{k,s}$ for the failure rate, λ_k.

Table 1. Wind speed categories

Wind speed category (s)	Wind Speed Range
1	$0 \leq w_t < 0.2w_{99}$
2	$0.2w_{99} \leq w_t < 0.4w_{99}$
3	$0.4w_{99} \leq w_t < 0.6w_{99}$
4	$0.6w_{99} \leq w_t < 0.8w_{99}$
5	$0.8w_{99} \leq w_t < 1.0w_{99}$
6	$1.0w_{99} \leq w_t < 1.2w_{99}$
7	$1.2w_{99} \leq w_t < 1.4w_{99}$
8	$1.4w_{99} \leq w_t$

All historic wind induced faults can be compared to wind speeds at the time of the fault and be assigned to one of these categories. For each threat and wind category the correction factor, $c_{k,s}$, can be calculated by dividing the percentage of outages occurring in that wind category by the percentage of time spent in that category. Or as follows

$$c_{k,s} = \frac{p_{k,s}}{p_s} \quad (7)$$

Where, p_k is the proportion of faults due to threat k occurring in category s, and p_s is the proportion of time that the wind speeds are in category s. The term $p_{k,s}$ is calculated as an aggregate value for the entire region, rather than component specific. This must be done given the few number of faults per threat and wind category for individual components. An example of the proportions in 7 and their

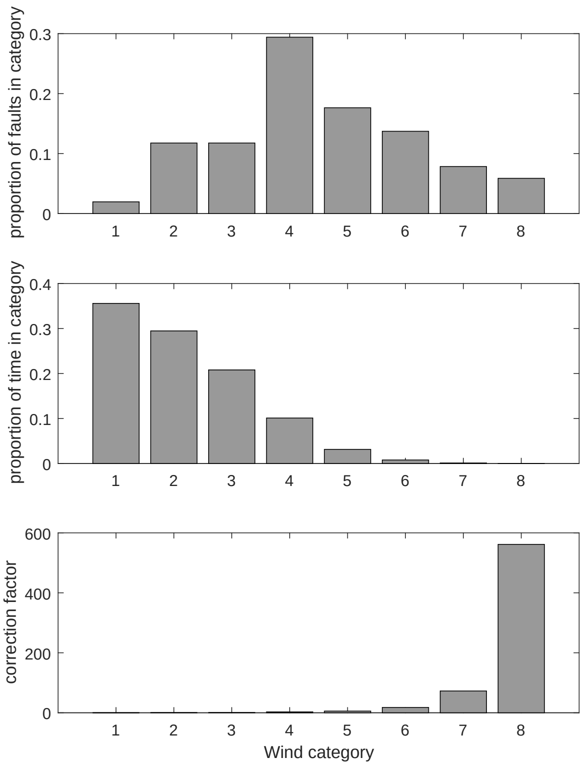

Figure 1. Example of correction factor calculation using Equation 7, for eight wind categories. Note that the proportion in the top figure is divided by the proportion in the second figure, to arrive at the correction factor in the third.

resulting correction factors for the threat of 'wind with ice load' are shown in Figure 1.

The three threat-specific failure rates, λ_0, λ_1, and λ_2, are calculated by partitioning the constant failure rate model based upon their cause, such that

$$\lambda_0 = \frac{\sum_t \{x_{k,t}|k=0\}}{T - \sum_j \{r_j|\psi_j = 0\}} \tag{8}$$

Where the term $\sum_t \{x_{k,t}|k=0\}$ denotes the number of faults, given that they were labelled to have an 'other' cause ($k=0$). Note that this condition is also applied to the correction in the denominator. Trivially, if all faults were deemed to be due to 'other' threats, then $\bar{\lambda}_k$ would be equal to λ_0. An additional adjustment is required for the remaining two threat-specific failure rates

$$\lambda_1 = \frac{\sum_t \{x_{k,t}|k=1\}}{T - \sum_0^T \beta_t - \sum_j \{r_j|\psi_j = 1\}} \tag{9}$$

$$\lambda_2 = \frac{\sum_t \{x_{k,t}|k=2\}}{\sum_0^T \beta_t - \sum_j \{r_j|\psi_j = 2\}} \tag{10}$$

Where the term $\sum_t \beta_{t,k}$ defines the number of periods of time in which icing events are credible. Note that in the formula for λ_1 this term is subtracted from T given that wind faults with no icing are only credible when icing is not credible. The annual average threat-specific failure rates can be calculated as

$$\bar{\lambda}_1 = \left(1 - \frac{\sum_t \beta_t}{T}\right) \sum_s c_{1,s} p_s \lambda_1 \tag{11}$$

$$\bar{\lambda}_2 = \left(\frac{\sum_t \beta_t}{T}\right) \sum_s c_{2,s} p_s \lambda_2 \tag{12}$$

Equations 11 and 12 can then be directly related back to the constant failure rate as

$$\bar{\lambda} = \lambda_0 + \bar{\lambda}_1 + \bar{\lambda}_2 \tag{13}$$

Therefore the variable failure rate model does not suggest that a component is more or less reliable than the constant failure rate model over the long-term, but redistributes the reliability in the short-term given the presence of exogenous threats.

The failure rate over any period of time can be assumed to be quasi-static, such that the exponential probability distribution can be used to estimate the failure probability, as in Billinton and Allan (1992), as

$$Q(t) = 1 - e^{\lambda t} \tag{14}$$

where $Q(t)$ defines the probability of a failure before the time interval $[0,t]$ has elapsed.

Failure rate model comparison

The effectiveness of the constant failure rate model with the described variable failure rate model, is compared using real-world fault data, and weather data covering a 10 year period. The weather data has been split into an 8 year training set (2005-2012), and a 2 year test set (2013-2014). These sets contain approximately 70,000 and 18,000 data points, respectively. The training set contains 74 faults, whilst the test set contains 22 faults.

The models are compared for a small region of the Icelandic transmission system. The names of the region and the studied components, and the units of some results, have been obscured deliberately for system security.

Given that the failure rate and outage probabilities are not directly measurable, it is not possible to directly measure the accuracy of any failure rate model unless the model is predicting an outage, or lack of, with certainty. The probabilistic prediction of outages is essentially a classification problem. Therefore the two failure rate models are compared using the cross-entropy error method. The accumulated cross-entropy error (ACE) function, also known as the log error function, is

$$ACE = \frac{-1}{N} \sum_{n=1}^{N} [y_n \log \hat{y}_n + (1 - y_n) \log(1 - \hat{y}_n)] \tag{15}$$

Where y_n is the n^{th} observation, and $\hat{y}_n$ is the n^{th} value predicted by the model, given N total observations.

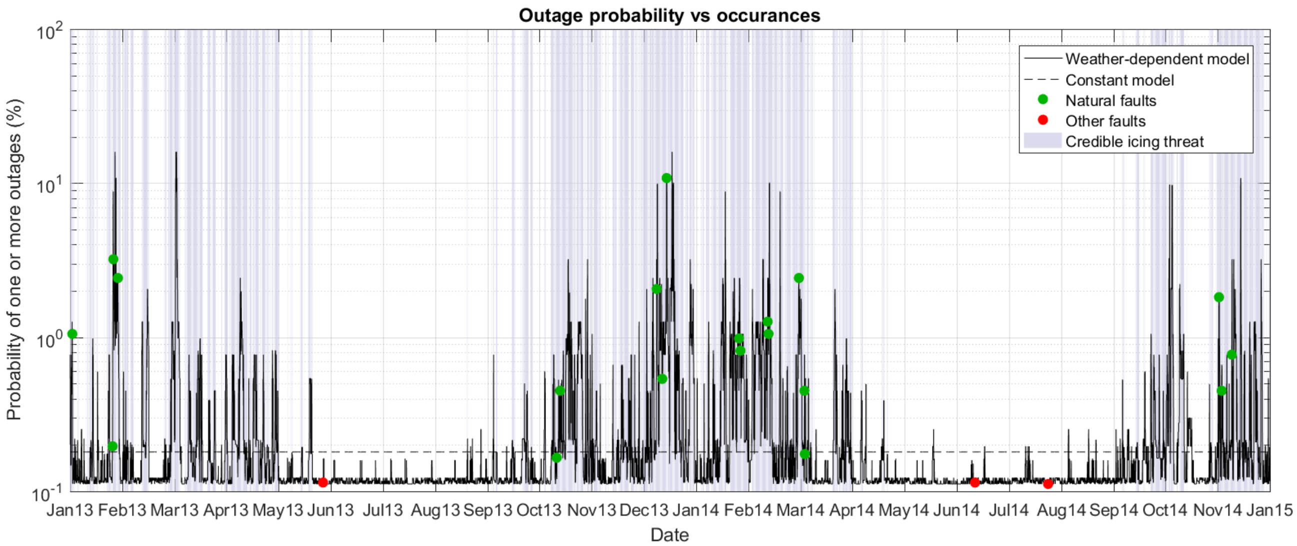

Figure 2. Comparison of the two failure rate models over two years of hourly weather data, shown as the probability of one or more outages in a given hour (note: logarithmic y-axis).

The observations are a binary vector where a value of 1 denotes an outage, and a value of 0 denotes no outage, for a given hour. The predictions, $\hat{y}_n$ are hourly failure probabilities calculated using the failure rate models. The ACE measurements aggregated over the entire region are shown in Table 2.

Table 2. Accumulated cross-entropy errors for the two failure rate models

	Constant λ	Weather-Dependent λ
Training Set	0.0040	0.0046
Test Set	0.0214	0.0212

The ACE is similar for both models, in both data sets, suggesting that there is no difference between the models in their ability to predict outages. This is largely due to the heavy bias of the data set, in which only 0.02% of data points contain an outage. The output of the model can be better understood by the visual comparison of the two failure rate models shown in Figure 2, over the test data set. The dashed line barely above the x-axis represents the constant failure rate model, whilst the solid line represents the weather-dependent failure rate model. The vertical grey lines colouring the background of the figure identify hours in which icing events were credible. The variability in the weather-dependent model is a function of both wind speed and icing credibility, as defined by Equation 4.

From this comparison it is apparent that the variable failure rate model is highly sensitive to the weather input data, showing large spikes in outage probabilities during storms with high winds and in which icing events are credible. The natural outages are clustered around these spikes, with no natural faults occurring in the summer period. Explicitly the natural outages are those due to wind and/or icing. The off-set outages occurring before or after storms (rather than during) are most likely a result of using only two locations for weather data to cover the region. Therefore the location of a fault may be significantly far from the location of the weather data used to explain it. This leads to both errors in timing and intensity. It is expected that these errors can be significantly corrected by using higher resolution weather data.

The two sets of correction factors determined in this study are compared with the Norwegian values determined in Tollefsen et al. (2015) in Figure 3. The credibility of icing was not considered in the Norwegian study, and therefore only one set of correction factors was produced. Note that there is no correction factor for c_1 for wind category 8, given that there are no occurrences in the data set of category 8 wind speeds without icing being a credible threat.

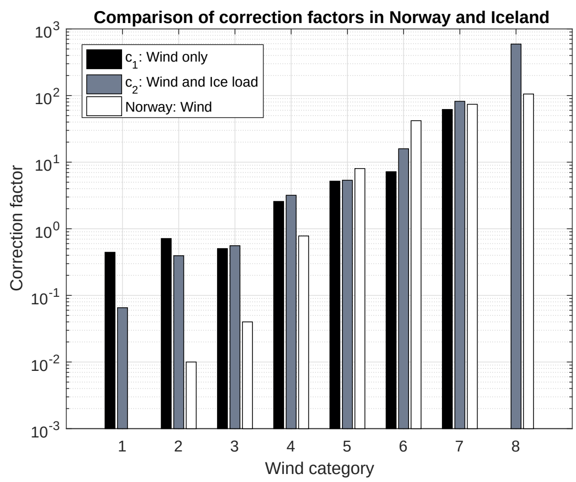

Figure 3. Comparison of the variable failure rate correction factors for the Norwegian and Icelandic models (Norwegian data from Tollefsen et al. (2015))

The correction factors for the Norwegian transmission system are clearly different to the Icelandic system, particularly for the extreme wind speed categories. The presence of faults in Iceland in the first wind category (0 to 0.2 times the 99% wind speed) is likely due to the lack of high resolution weather data.

Effect on system risk estimates

Failure rate models are used for the estimation of outage probabilities, but it is difficult to interpret this information without considering the consequences of any outage. In the context of real-time power system operation, the major consequences are service outages and the period over which they extend. The estimation of consequences requires a tool, as discussed in the background section. In this section we test the sensitivity of Promaps online to the use of the variable failure rate model, applied to a region of the Icelandic transmission system.

This test covers a week of operation in both Summer and Winter, with an hourly time resolution. Given that there are two cases, two models, and 168 hours per case, this requires 672 individual simulations. The maintenance test case required a further 336 simulations, for a total of 1008 simulations. Each simulation required 5000 power-flow calculations, one for each considered contingency, as the entire power system was simulated to properly capture the risk of import/export into the region. Therefore approximately 5 million power-flow calculations were required to perform this study.

The consequence of outages are quantified in terms of System Minutes (SMS), as defined by Icelandic Ministry of Industry (2004) as

$$SMS = \frac{\sum_i E_i}{E}(8760).(60) \tag{16}$$

With units of minutes per year. The terms E_i and E are the unserved energy of outage i and the total energy demanded by customers in the region over the outage period, respectively, both in units of megawatt-hours. This measures the loss of service over some duration, in terms of losing the entire system for some duration of minutes to arrive at the same quantity of energy not served. The expected SMS can be used as a risk metric for the power system, calculated as

$$Risk = \mathbb{E}[SMS] = \sum_c \pi_c.SMS_c \tag{17}$$

Where π_c and SMS_c are the probability of some contingency c and its consequence in terms of SMS, respectively. The expected SMS for the two test cases, for both failure rate models, are shown in Figure 4.

The variation in risk when applying the constant failure rate model is due to spatiotemporal variations in production and consumption of energy. In the Summer case, the risk is similar in both models, but with the weather-dependent model resulting in a mean expected SMS that is 22 minutes lower (33% smaller). This is due to the weather-dependent model excluding faults due to icing (as icing is not credible during the studied period) and the wind speeds being in low wind speed categories (correction factors less than 1).

The Winter case shows a maximum risk of 590 system minutes (compared to a Summer maximum of 82 minutes) and greater variability than the constant failure rate model. Notably the risk is far more sensitive to the spatiotemporal variation in weather rather than load or generation. The mean risk in the Winter case is higher than the Summer case for both models.

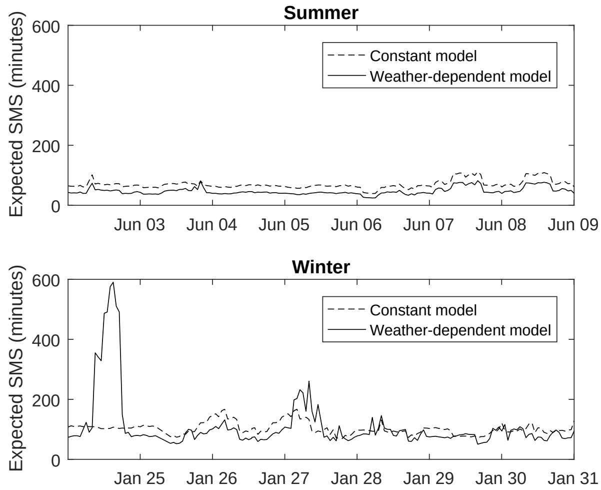

Figure 4. Expected SMS of a region of the Icelandic power system, over a week-long period in Summer and Winter, using a constant or weather-dependent failure rate model.

The sensitivity of the model to weather-dependent failure models is amplified by the presence of maintenance activities, as shown in Figure 5. During the Summer, if a particular line is disconnected for maintenance, the risk is multiplied by a factor of 2.4 for both models. Using the weather-dependent failure rate model, the risk during maintenance is not considerably higher than the maximum risk in the days before or after maintenance. However this may not be the case for all maintenance activities. In this particular case, the high risk identified by the constant failure rate model may be unacceptable, but the risk given by the probabilistic model may be considered reasonable. This simply highlights that if probabilistic risk assessments are used to inform maintenance outage plans, that weather-dependence can significantly affect the conclusions.

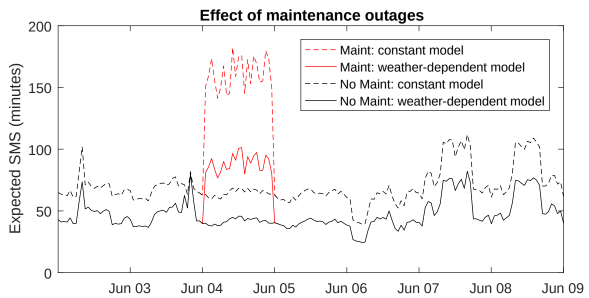

Figure 5. Expected SMS of a region of the Icelandic power system in Summer, given the outage of a single line over one day for maintenance

The impact of weather-dependent failure rates on the distribution of risk is shown in Figure 6. In the Summer case the use of a weather-dependent failure rate model offsets the expected SMS by -20 minutes. Most hours in the Winter case experience the same offset, with the exception of a long tail of high risk periods.

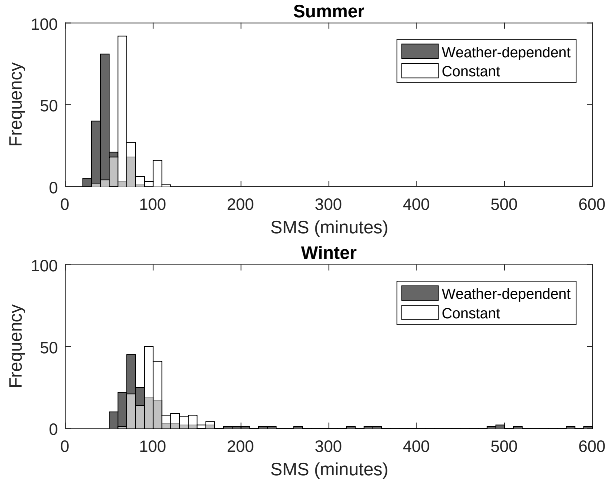

Figure 6. Distribution of Expected SMS values for the Winter and Summer cases, for constant and weather-dependent failure rate models. Overlapping portions of the distributions are shown in grey.

Discussion

This study has shown an example application of a variable failure rate model on a region of a real-world power system, using operational data and weather data, and tested the sensitivity of these models on a state-of-the-art probabilistic reliability tool. Although the weather-dependent failure rate model is not significantly different from the constant failure rate model in terms of cross-entropy error, the apparent clustering of faults around spikes in outage probability (in Figure 2) suggests that the model reflects natural variability more than the constant failure rate model.

As stated in this paper, TSOs previously identified the need for weather-dependent probabilistic models in reliability assessments. In the two test cases, the inclusion of weather-dependent outages greatly increased the sensitivity of the risk indicator. This sensitivity may increase further with improved weather data resolution, and improved failure rate modelling. It should also be noted that fault statistics have not been historically recorded for the purpose of failure rate modelling, leading to some inconsistent labelling of fault causes. The mislabelled causes would likely result in reduced model sensitivity, and erroneous correlations between exogenous variables and outages. Such errors can be avoided by relabelling threats as 'unknown' for outages that are not supported by recorded descriptions or photos of the underlying fault.

The accuracy and sensitivity of the failure rate models not only depends on data resolution, but also on the model structure and the number of threats considered. Inclusion of more threats and explanatory variables should increase model sensitivity and accuracy. Care should be given however to the treatment of dependence between explanatory variables, as observed with the larger correction factors for wind when icing is credible. Additional variables, such as wind direction, would correlate with wind speed and icing credibility, whilst lightning strikes may be modelled independent of wind or icing. Other threats, such as sabotage, may also be included in failure rate modelling through expert inputs.

At present the installation of Promaps at Landsnet calculates the system minutes every 5 minutes, based on inputs of system topology, nodal load, nodal generation, nodal spinning reserves, and contingencies (and combinations of). This includes a system response model in the form of a power-flow calculation including heuristic corrective controls and system protection. There are future plans to include weather-dependency in the software, based on developing the method presented in this paper.

Conclusion

The real-world comparison made in this paper between constant and variable failure rate models provides further support to existing literature and TSO feedback on the importance of including weather-dependence in risk calculations. The observed clustering of faults around spikes in outage probabilities suggests that variable failure rate models may be of value in predicting periods of high risk. Observed sensitivities in state-of-the-art risk assessment software to variable failure rates highlight the importance of considering weather-dependence of outages.

The variable failure rate model estimates that the risk taken during summer maintenance activities in the region is of negligible difference compared to median winter risk levels. Finally, the use of the variable model results in the distribution of risk in winter becoming positively skewed, rather than normally distributed, due to a high number of rare high impact events. The further development of weather-dependent failure rate models and use of higher resolution weather data is anticipated to lead to more accurate and sensitive outage probability modelling. In practice this may lead to greater operator awareness to exogenous threats to the power system, and hence to a more reliable power system.

Acknowledgements

The authors would like to acknowledge the Technical University of Denmark (DTU) for providing the weather data used in this study.

The authors would also like to acknowledge Landsnet for providing data related to their power system, and Goodtech for allowing use and modification of Promaps for this research.

Declaration of conflicting interests

Potential conflicts of interest. A.B.S. and T.T. are employed by Goodtech, the developer of Promaps. All other authors report no conflicts of interest relevant to this paper.

Funding

The research leading to these results has received funding from the European Union Seventh Framework Programme (FP7/2007-2013) under grant agreement n^{o} 608540.

References

Alvehag, K. and Soder, L. (2011), 'A reliability model for distribution systems incorporating seasonal variations in severe weather', *IEEE Transactions on Power Delivery* **26**(2), 910–919.

Azevedo, F., Gomes-Mota, J., Campos-Pinto, L., Machado, N. and de Graaff, S. d. A. (2015), 'Ohl assessment and risk evaluation based on environmental and inspection data', *International Journal of Electrical Power & Energy Systems* **70**, 127–130.

Billinton, R. (1972), 'Bibliography on the application of probability methods in power system reliability evaluation', *IEEE Transactions on power Apparatus and systems* (2), 649–660.

Billinton, R. and Acharya, J. (2006), 'Weather-based distribution system reliability evaluation', *IEE Proceedings-Generation, Transmission and Distribution* **153**(5), 499 – 506.

Billinton, R. and Allan, R. (1996), *Reliability Evaluation of Power Systems*, Plenum Press.

Billinton, R. and Allan, R. N. (1992), *Reliability evaluation of engineering systems*, Springer.

Billinton, R. and Wenyuan, L. (1991), 'A novel method for incorporating weather effects in composite system adequacy evaluation', *IEEE Transactions on Power Systems* **6**(3), 1154–1160.

Bollen, M. H. (1993), *Literature search for reliability data of components in electric distribution networks*, Eindhoven University of Technology, Faculty of Electrical Engineering.

Capitanescu, F. (2016), 'Critical review of recent advances and further developments needed in ac optimal power flow', *Electrical Power Systems Research* **136**, 57–68.

Digernes, T., Svensen, A., Aabo, Y., Hernandez, C. and Palsson, M. (2007), Analyses of delivery reliability in electrical power systems, *in* 'Risk, Reliability and Societal Safety', CRC Press, pp. 2289–2296.

Eliasson, A. (2005), 'Natural hazards and the icelandic power transmission grid', *7. konf. slovenskih elektroenergetikov* .

Endrenyi, J. (1978), *Reliability modeling in Electric Power Systems*, Wiley.

ENTSO-E (2009), 'Continental europe operation handbook p3 - policy 3: Operational security'.

GARPUR consortium (2014*a*), 'D1.1 Current practices, drivers and barriers for new reliability standards'.

GARPUR consortium (2014*b*), 'D1.2 State of the art on reliability assessment in power systems'.

Henneaux, P. and Kirschen, D. S. (2016), 'Probabilistic security analysis of optimal transmission sitching', *IEEE Transactions on Power Systems* **31**(1), 508–517.

Icelandic Ministry of Industry (2004), 'Regulation on the quality of electricity and security of supply'.
URL: *http://www.reglugerd.is/reglugerdir/allar/nr/1048-2004*

Karangelos, E. and Wehenkel, L. (2016), Probabilistic reliability management approach and criteria for power system real-time operation, To appear in 19th Power System computation Conf. (PSCC 2016).

Kirschen, D. S. and Jayaweera, D. (2007), 'Comparison of risk-based and deterministic security assessments', **1**(4), 527–533.

Lemaitre, C. and Panciatici, P. (2014), itesla: Innovative tools for electrical system security within large areas, *in* '2014 IEEE PES General Meeting— Conference & Exposition', IEEE, pp. 1–2.

López, P. C., Sadikovic, R., Pinto, H. and Magnago, F. (2015), Swiss tso experience with an ac security-constrained optimal power flow application for real-time security management, *in* 'PowerTech, 2015 IEEE Eindhoven', IEEE, pp. 1–6.

Machado, N., de Graaff, S. A. and Pestana, R. (2014), Risk assessment methodology Running tests at the Portuguese TSO, CIGR, Paris, France.

Makkonen, L. (2000), 'Models for the growth of rime, glaze, icicles and wet snow on structures', *Philosophical Transactions of the Royal Society of London A: Mathematical, Physical and Engineering Sciences* **358**(1776), 2913–2939.

Panciatici, P., Bareux, G. and Wehenkel, L. (2012), 'Operating in the fog: Security management under uncertainty', *IEEE Power and Energy Magazine* **10**(5), 40–49.

Perkin, S., Bjornsson, G., Baldursdottir, I., Pallson, M., Kristjansson, R., Stefansson, H., Jensson, P., Karangelos, E. and Wehenkel, L. (2016), Framework for threat based failure rates in transmission system operation, *in* '2016 Second International Symposium on Stochastic Models in Reliability Engineering, Life Science and Operations Management (SMRLO)', IEEE, pp. 150–158.

Pourbeik, P., Kundur, P. S. and Taylor, C. W. (2006), 'The anatomy of a power grid blackout', *IEEE Power and Energy Magazine* **4**(5), 22–29.

Tollefsen, T., Svendsen, A., Pedersen, R., Skeie, P., Lunde, T. and Maelan, J. (2015), Online reliability calculations of power systems with forecasted and real time weather influence, *in* 'Safety and Reliability of Complex Engineered Systems', CRC Press, chapter 215, pp. 1739–1744.

UMBRELLA consortium (2016), 'D1.2 Toolbox for Common Forecasting, Risk Assessment and Operational Optimisation in Grid Security Cooperations of Transmission System Operators'.

Vefsnmo, H., Kjolle, G., Jakobsen, S. H., Ciapessoni, E., Cirio, D. and Pitto, A. (2015), Risk assessment tool for operation: from threat models to risk indicators, *in* 'PowerTech, 2015 IEEE Eindhoven', IEEE.

Zhang, Y., Wang, L., Xiang, Y. and Ten, C.-W. (2015), 'Power system reliability evaluation with scada cybersecurity considerations', *IEEE Transactions on Smart Grid* **6**(4), 1707–1721.